Analyst

ROYAL SOCIETY OF CHEMISTRY

PAPER

View Article Online
View Journal | View Issue

Cite this: *Analyst*, 2021, **146**, 2248

A site-specific DNA methylation biosensor for both visual and magnetic determination based on lateral flow assay†

Jiaxing Zhang, ‡ Xiaonan Liu, ‡ Sinong Zhang, Yu Cai, Kang Ma, Kai Hua and Yali Cui *

Received 25th November 2020,
Accepted 1st February 2021

DOI: 10.1039/d0an02277b

rsc.li/analyst

Tumorigenesis driven by abnormal DNA methylation has highlighted the need to develop a portable, rapid and sensitive strategy for accurate methylation detection with a specific cancer-prognostic gene, which caters to the popularization of precision medicine. In this study, a site-specific biosensor for both visual and magnetic DNA methylation determination has been established based on lateral flow assay. By introducing digoxin- and biotin-labeled primers into PCR, the amplicons can be recognized and captured by gold magnetic nanoparticles (GMNPs) in this biosensor. Working as a signal probe, the optical property of GMNPs allows the amplicons to be interpreted with naked eyes avoiding any complex equipment and cumbersome operation after PCR. Moreover, by virtue of the magnetic property of GMNP, the signal can be explained and recorded by a magnetometer in clinical practice. The introduction of tailor-made primer sets makes it possible to accurately distinguish 0.1% methylated variants in the presence of numerous unmethylated variants as strong interferential background and *vice versa* at target cytosine–guanine dinucleotide. A distinct signal can be observed with as low as 0.01 pg variants for both visual and magnetic analyses. As a significant tumor suppressor gene, the promoter methylation status of miR-34a is accurately determined with not only cell lines but also with clinical samples, which demonstrates the great potential of this biosensor for cancer diagnosis and prognosis.

1. Introduction

DNA methylation, a primary epigenetic modification, is strongly involved in the regulation of gene expression without the alteration of nucleotide sequence in mammalian species.[1,2] Aberration in DNA methylation, particularly in the promoter of a cancer-prognostic gene, is a significant marker in tumorigenesis from clinical perspective.[3,4] As a promising diagnosis index for clinical practice, DNA methylation has served as a predictive biomarker for cancer diagnosis and prognosis.[5,6]

Along with revealed cancer-related DNA methylation patterns, DNA methylation determination has attracted extensive attention, leading to establishment of numerous methods dedicated to its clinical practice.[7–12] In general, three strategies are adopted for these methods, namely restriction enzyme digestion,[13,14] affinity enrichment[15–17] and bisulfite conversion.[18–20] The restriction enzyme digestion-based methods determine the status of DNA methylation through digesting cytosine–guanine (CpG) dinucleotide while leaving the methylated CpG dinucleotide intact.[21] However, this strategy restricts the exploration of desired sites because of the limitation of the restriction enzyme. The affinity enrichment-derived methods recognize methylated DNA by the methyl-CpG-binding domain.[22,23] However, this strategy cannot locate the target CpG dinucleotide. The bisulfite conversion-based methods, the most widely investigated strategy, translate methylation discrepancy into sequence discrepancy by converting cytosine to uracil leaving methylcytosine unchanged,[24] which facilitates numerous sequence determination technologies to be integrated for locating any desired CpG sites. Taking this advantage, a variety of bisulfite conversion-based methods have been developed for site-specific DNA methylation identification, such as methylation-specific PCR,[25] real-time fluorescent quantitative methylation-specific PCR,[26] methylation-sensitive high-resolution melting,[27–29] capillary electrophoresis[30] and microarrays.[31] Although the site-specific DNA methylation status can be accurately determined, the sophisticated and expensive instruments, or cumbersome operations hinder the application of these methods in basic

College of Life Sciences, Northwest University, Xi'an, 710069, China.
E-mail: yalicui@nwu.edu.cn

†Electronic supplementary information (ESI) available. See DOI: 10.1039/d0an02277b

‡Contributed equally.

medical institution as well as for the popularization of precision medicine. In order to facilitate cancer diagnosis and prognosis for clinical oncology, a portable and rapid strategy for site-specific DNA methylation identification is highly desirable.

A lateral flow assay (LFA), a portable and rapid biomarker detection device integrated into a mini dimension, has been extensively applied in point-of-care testing (POCT) such as the detection of pathogens[32,33] and genotyping,[34,35] which indicates its significant potential for clinical diagnosis. Xu *et al.* were the first in employing LFA to perform portable DNA methylation determination,[36] which could obtain the results from sequence discrepancy for about 150 min and 1% target variants could be distinguished under the interferential background.

Herein, a novel DNA methylation biosensor for specific CpG dinucleotide determination has been established based on LFA denoted as the methylation-specific lateral flow assay (MS-LFA). By introducing digoxin- and biotin-labeled primers, the detection result can be interpreted through recognition and conjugation between amplicons and gold magnetic nanoparticles (GMNPs) integrated in this biosensor. Working as a signal probe, GMNP provides not only optical signal, which allows result interpretation with naked eyes in 5 min avoiding any complex equipment and cumbersome operation after PCR, but also magnetic signal that records automatically with a magnetometer and computed result interpretation. The proposed method satisfies the POCT requirements for portability, rapidity and sensitivity, which make this biosensor a great potential for DNA methylation determination in clinical practice.

2. Experimental

2.1. Oligonucleotides

As a demonstrated, miR-34a, a significant tumor suppressor gene,[37–41] was chosen as the model for MS-LFA establishment. For convenience, the methylation status was noted as "M" and unmethylation status was noted as "U". Two specific primer sets were designed to distinguish the promoter methylation status of miR-34a at the specific CpG dinucleotide site including two biotin-labeled specific primers and one digoxin-labeled common primer (M primer set to recognize the methylated variant and U primer set to recognize the unmethylated variant) using the Primer 5.0 software program (Primer-E Ltd, Plymouth, UK). Besides, two other primers were also designed for bisulfite sequencing. The sequence of all the primers is shown in Table 1 and all the primers were synthesized by Invitrogen Biotechnology Ltd (Shanghai, PRC).

2.2. Plasmid construction and identification

Plasmids were constructed using a pMD19-T Vector Cloning Kit (Takara Bio Inc. Dalian, PRC) and were extracted from transformed *Escherichia coli* DH5α cells (Takara Bio Inc.). All the plasmids were identified by sequencing through TsingKe Biotech Ltd (Beijing, PRC), and the concentration was determined using a NanoDrop 2000 ultraviolet-visible spectrophotometer (Thermo Fisher Scientific, Wilmington, DE, USA).

Table 1 Primer sequences for MS-LFA and Bisulfite sequencing

Application	Primer	Sequence (5′–3′)
Bisulfite sequencing	Forward	GTGAAGGGGATGAGGATTAGGA
	Reverse	ACATCTCCTCCACCTAAAAAAAAA
MS-LFA	Common	GAAGGGGATGAGGATTAGGATTT
	Methylation-specific	ATAAAAACGACGCCAACACAG
	Unmethylation-specific	ACACATAAAAACAACACCAACACAA

2.3. Cell culture and clinical samples

Breast cancer cell lines (T-47D, MDA-MB-453 and Hs-578 T) were purchased from the Cell Bank of Chinese Academy of Sciences (Shanghai, PRC) and routinely cultured in a DMEM/F12 (1 : 1) medium (HyClone, Logan, UT, USA) containing 10% FBS (GeminiBio, West Sacramento, CA, USA) at 37 °C in a humidified atmosphere (95% air and 5% CO_2). Paraffin-embedded cancerous breast tissues from 5 breast cancer patients and non-cancerous breast tissues from 5 non-breast cancer patients were collected from Shanghai Histo Pathology Diagnostic Center (Shanghai, PRC) with informed consent. This research was approved by the Ethics Committee of the College of Life Sciences, Northwest University (Xi'an, Shaanxi, PRC). All operations were performed in accordance with the Helsinki declaration.

2.4. DNA extraction and bisulfite modification

Genomic DNA from the cells was extracted using a TIANamp Genomic DNA Kit (Tiangen Biotech Co., Ltd Beijing, PRC), while genomic DNA from tissues was extracted using a TIANquick FFPE DNA Kit (Tiangen Biotech Co., Ltd). The bisulfite modification of genomic DNA was performed using a EpiTect Bisulfite Kit (Qiagen, Hilden, Germany) according to the manufacturer's instructions.

2.5. MS-LFA design

MS-LFA contained two strategies including target DNA amplification by PCR and amplicons interpretation by an LFA device. For DNA amplification, two individual PCR amplification containing M and U primer sets, respectively, were performed simultaneously to determine the promoter methylation status of miR-34a at the specific CpG dinucleotide site. Both of the reaction mixtures with a final volume at a 50 μL containing 1× EpiTaq PCR Buffer (Takara Bio Inc.), 0.3 mM of each dNTPs (ShineGene, Shanghai, PRC), 2.5 mM $MgCl_2$ (Thermo Fisher Scientific), 0.625 U HotMaster Taq DNA Polymerase (Tiangen Biotech Co., Ltd), and 100 nM of each primer were incubated using a 2720 thermal cycler (Applied Biosystems, Foster City, USA) with the parameters: 5 min at 94 °C, 29 cycles of 10 s at 95 °C, 30 s at 59 °C and 30 s at 72 °C, and one step of 5 min at 72 °C.

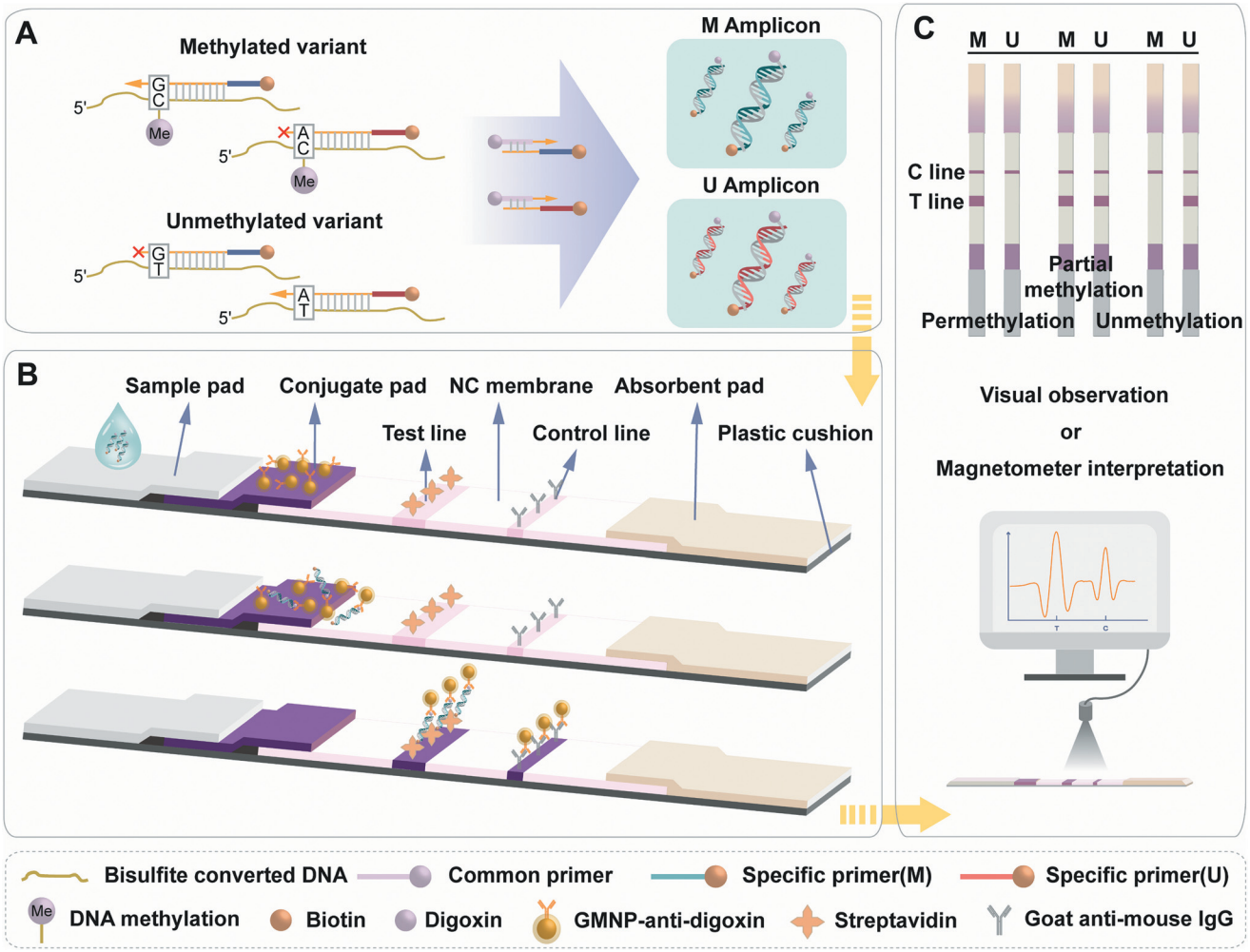

Fig. 1 Schematic of MS-LFA. (A) Primer sets and amplification process of target variants. (B) Structure of LFA and signal generation. (C) Methylation status identified with MS-LFA based on visual and magnetic interpretation.

For amplicons interpretation, an LFA device was employed that contained GMNP as the signal generator. The LFA device was assembled from five components including sample pad, conjugate pad, nitrocellulose membrane, absorbent pad and plastic cushion to interpret the amplicons (Fig. 1B). GMNP was synthesized and conjugated with the digoxin antibody according to a previous report,[42] which was sprayed onto the conjugate pad using a BioJet HM3010 dispenser (BioDot Inc., California, USA). Streptavidin (Promega Biotech Inc., Madison, WI, USA) and goat anti-mouse IgG (Joey Bioscience Inc., Shanghai, PRC) were immobilized in the defined test line (T line) and control line (C line) on the nitrocellulose membrane, respectively. All reaction solutions were pipetted onto the sample pad of LFA after PCR was complete.

The signal presentation in this biosensor depended on the bridge connection of amplicons between GMNP and streptavidin immobilized on the T line, which indicated the presence of target amplicons. The target DNA methylation status could be interpreted *via* both the naked-eye and a magnetometer (Magna Bio Sciences, USA). Moreover, the performance of MS-LFA was optimized with different concentrations of primer (60, 80, 100, 120 and 140 nM), annealing temperatures (57, 58, 59, 60 and 61 °C) and cycle numbers (28, 29, 30, 31 and 32 cycles).

2.6. Bisulfite sequencing

The promoter fragment of miR-34a was amplified with the bisulfite-modified genomic DNA as the template, and the fragment was embedded into the pMD19-T Vector subsequently and transformed into *Escherichia coli* DH5α cells. Five positive recombinant clones of each sample were selected randomly for sequencing by TsingKe Biotech Ltd.

3. Results and discussion

3.1. MS-LFA design

Two specific primer sets were tailor-made to achieve the best discrimination between methylated and unmethylated variants. In order to increase the specificity of this biosensor, an

additional mismatch was introduced at the 3′-penultimate base of each specific primer according to the principle of the amplification-refractory mutation system. The candidate primers were selected through the thermodynamic analysis to maximize the coupling between the matched primer and variant but hinder the coupling between unmatched primer and variant. According to the Primer 5.0 software program, the selected primers varied greatly in the standard free energy, reflecting the specificity of primer sets to distinguish the methylated and unmethylated variants.

Two individual PCR amplifications containing M and U primer sets, respectively, were performed simultaneously to determine the target CpG dinucleotide methylation status of each specimen. Taking advantage of the amplification-refractory mutation system, the amplicons were produced only when the 3′-terminus of the specific primer is completely complementary to the corresponding variant (Fig. 1A). Thus, whether the amplicons produced or not could indicate the DNA methylation status directly. Therefore, an LFA device was employed in this biosensor. By introducing digoxin- and biotin-labeled primers, the amplicons could be recognized and conjugated by GMNP-anti-digoxin once the reaction solution was pipetted onto the sample pad of LFA after PCR (Fig. 1B). Driven by the capillary force, the amplicon-GMNP complexes migrated along the nitrocellulose membrane and aggregated on the T line *via* the conjugation between biotin-labeled amplicons and streptavidin. Excess GMNP-anti-digoxin migrated along the nitrocellulose membrane continually and aggregated on the C line through the conjugation between the digoxin antibody and goat anti-mouse IgG, demonstrating the validity of this biosensor. Based on the optical and magnetic property of GMNP, the aggregation of GMNP provided two signal forms for result interpretation. The optical signal allowed the result interpretation by visual observation, while the magnetic signal allowed the result interpretation by magnetometer automatically (Fig. 1C).

The determination of the DNA methylation status was based on the signal generation by the LFA device from the M and U reaction mixture. When the signal presented on the T line came only from the M reaction, it indicated the permethylation status. In contrast, the signal observed only on the T line from the U reaction mixture pointed out the unmethylation status. However, a signal showing on both T lines communicated the partial methylation status of tested specimen (Fig. 2A and B). Besides, the threshold value for positive result interpretation by magnetic determination was defined

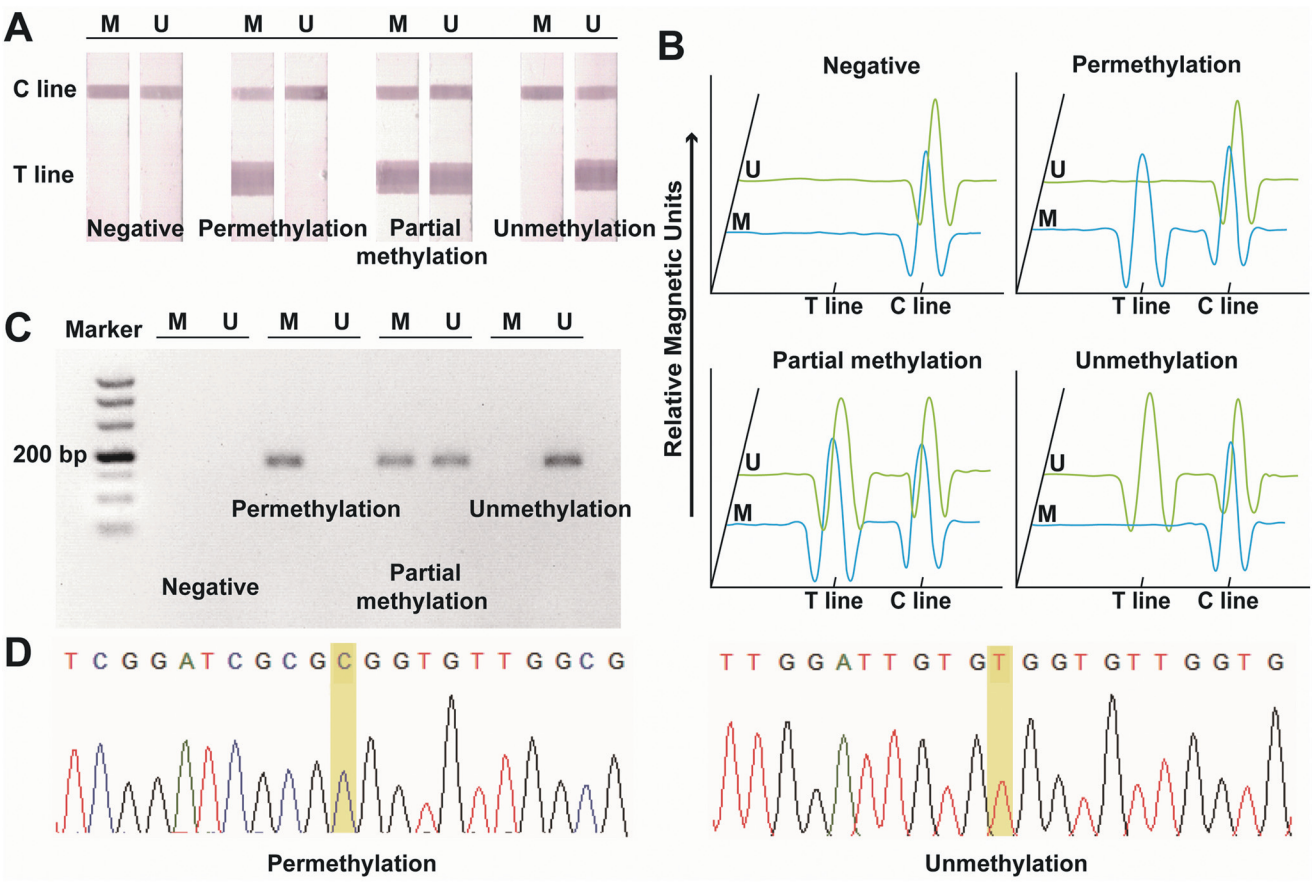

Fig. 2 Methylation status identification results. Identification result provided by (A) MS-LFA through visual interpretation, (B) MS-LFA through magnetometer, automatically, (C) electrophoresis and (D) bisulfite sequencing.

(Fig. S1†). Moreover, comparison with the identification results of electrophoresis (Fig. 2C) and bisulfite sequencing (Fig. 2D) indicated that this biosensor has the same accuracy as standard method for the DNA methylation status determination.

3.2. MS-LFA optimization

For preliminary development of MS-LFA, the plasmids containing bisulfite-modified promoter sequence of miR-34a were used as the standard sequence control. The performance of MS-LFA was evaluated with a series of primers at different concentrations. When the primer concentration was lower than 80 nM, the amplification could not produce enough amplicons for signal observation. However, distinct tinctorial bands were observed on the T line for the accurate result determination with other primer concentrations (Fig. S2A†). Finally, 100 nM was selected as the optimal concentration in MS-LFA to ensure the specificity of this biosensor. The influence of the annealing temperature for this biosensor was also evaluated. A non-specific signal was observed at and below 57 °C, while accurate the result was obtained with other tested temperatures (Fig. S2B†). Thus, 59 °C was chosen to balance the specificity and sensitivity of this method. For the thermal cycle, the non-specific signal was observed with 32 cycles, while no obvious difference was observed among other tested cycles (Fig. S2C†). Hence, 29 cycles were selected in order to reduce the turn-around time.

3.3. Performance evaluation of MS-LFA

To evaluate the performance of this biosensor, a series of plasmid mixtures containing 1%, 0.5%, 0.1% and 0% target variants, respectively, with a final concentration at 10 pg were prepared to determine the specificity and sensitivity of MS-LFA. The signal intensity of the T line increased gradually along with the increasing concentration of target variants, and no signal was generated with 100% unmatched variants (Fig. 3). Therefore, as few as 0.01 pg target variants could be accurately distinguished under the strong interferential background with both visual and magnetic determination.

3.4. Cell lines and clinical samples analysis with MS-LFA

In order to evaluate the ability of this biosensor for actual specimen, the promoter methylation status of miR-34a was determined with genomic DNA extracted from breast cancer cell lines. The unmethylation status was found with T-47D and MDA-MB-453, while the permethylation status was observed at the target CpG site with Hs-578 T. Moreover, the determination results of all cell lines using MS-LFA were consistent with those provided by bisulfite sequencing, and the most authoritative method for the DNA methylation analysis, which indicated that this biosensor could accurately discriminate the original DNA methylation pattern (Fig. 4). In addition, 5 cancerous and 5 non-cancerous breast tissues were taken as actual clinical samples for the analysis. Among the 10 specimens, 3 cases had optical signal only from the U reaction mixture and the signal was observed from both M and U reaction mixtures

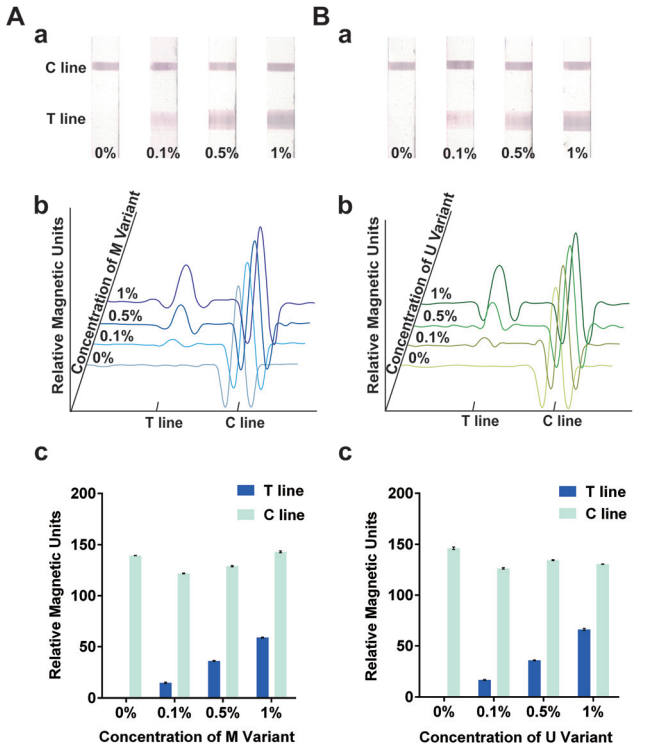

Fig. 3 The signal intensity of MS-LFA with different proportions of target variant. (A) The signal intensity of MS-LFA with combination of methylated primer set and different proportions of methylated variant diluted in unmethylated variant ((a) The brightness of T line and C line, (b) Curve graph of magnetic signal on LFA, (c) Magnetic signal peak value of T line and C line). (B) The signal intensity of MS-LFA with combination of unmethylated primer set and different proportions of unmethylated variant diluted in methylated variant ((a) the brightness of T line and C line, (b) curve graph of magnetic signal on LFA, (c) magnetic signal peak value of T line and C line).

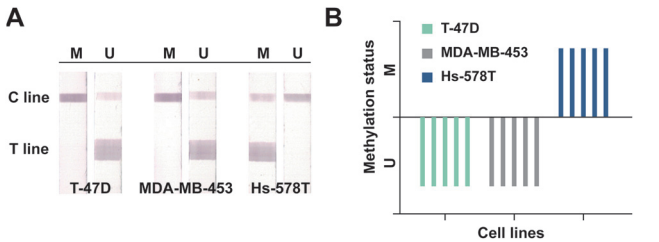

Fig. 4 Methylation status identification result with cell lines. Identification result provided by (A) MS-LFA and (B) bisulfite sequencing with cell lines.

for the remaining 7 cases, which indicated 3 unmethylated specimens and 7 partially methylated specimens (Fig. S3†).

Considering the great potential of DNA methylation detection for cancer diagnosis and prognosis, developing a portable, rapid and sensitive strategy for site-specific methylation determination is desired for the popularization of precision medicine. Although numerous DNA methylation identification techniques have been developed such as sequencing-based methods,[43] fluorescence-based methods[26] and electro-

chemical-based methods,[44,45] the time-consuming process and cumbersome manual operation are required as well as the sophisticated instruments, which severely hinder their application for clinical practice. In order to simplify the operation and minimize the device, LFA, a portable and rapid biomolecule detection device integrated into a mini dimension, was first introduced by Xu *et al.* for DNA methylation detection, which enables the detection result to be obtained in a more convenient way.[36] However, this method not only requires over 150 min to obtain the result from sequence discrepancy, but also merely 1% target variants can be distinguished under the interferential background. Thus, although this method blazes a trail to perform portable DNA methylation identification, the timely diagnosis information for clinical oncology and the determination of trace biomarkers in highly heterogeneous specimens are hardly achieves. In the present research, by taking advantage of bio-labeled oligonucleotides, the amplicons could be interpreted by a portable mini device within 5 min dispensing with any complex instrument and cumbersome operations, which makes the site-specific DNA methylation status to be accurately determined by this novel biosensor from sequence discrepancy within 90 min. As a signal generator in MS-LFA, GMNP contains both optical and magnetic properties, which equips this biosensor with two signal forms for data interpretation. The optical signal allows us to obtain the result with naked-eyes, while the magnetic signal facilitates the analysis for larger sample in clinical practice.

The trace of the biomarker in the early stage of tumorigenesis extremely yearns a highly sensitive strategy for cancer diagnosis and prognosis. However, the colloidal gold-based lateral flow assay such as the method mentioned above can only provide optical signal generated by the colloidal gold aggregated on the surface of the porous nitrocellulose membrane,[36] which mutes their sensitivity gravely. Owing to the magnetic property of GMNP, all aggregated GMNPs are responsible for magnetic signal generation, which makes this biosensor achieve a high sensitivity. Moreover, by introducing additional mismatch nucleobases, the tailor-made primer sets increase the specificity and sensitivity further, which makes it possible to accurately detect as low as 0.01 pg target variants under the strong interferential background for both visual and magnetic interpretations. The promoter methylation status of miR-34a, for instance, is accurately determined with cell lines and actual clinical samples, which indicate the great potential of this biosensor for cancer diagnosis and prognosis. As a general DNA methylation detection platform, this biosensor can be easily extended to any other desired biomarkers by tailor-made primer sets redesigned.

Conclusions

In summary, a site-specific methylation biosensor has been established, which enables single-locus DNA methylation determination with both visual and magnetic interpretations. This biosensor not only achieves high sensitivity, specificity and speediness but also avoids any expensive and sophisticated instruments or complicated operations. The performance of this biosensor has been verified with real-world samples in the determination of DNA methylation patterns of the miR-34a promoter, which indicates the great potential of this DNA methylation biosensor for cancer diagnosis and prognosis.

Author contributions

Jiaxing Zhang: conceptualization, methodology, investigation, data curation, writing-original draft. Xiaonan Liu: conceptualization, methodology, investigation, writing- review and editing. Sinong Zhang: data curation. Yu Cai: data curation. Kang Ma: data curation. Kai Hua: writing- review and editing. Yali Cui: resources, supervision, funding acquisition.

Conflicts of interest

There are no conflicts to declare.

Acknowledgements

This research was supported by the National Natural Science Foundation of China (No. 81772289).

References

1 L. D. Moore, T. Le and G. Fan, *Neuropsychopharmacology*, 2013, **38**, 23–38.
2 Y. Dor and H. Cedar, *Lancet*, 2018, **392**, 777–786.
3 M. Klutstein, D. Nejman, R. Greenfield and H. Cedar, *Cancer Res.*, 2016, **76**, 3446–3450.
4 W. Zhang and J. Xu, *Biomark. Res.*, 2017, **5**, 1.
5 H. Heyn and M. Esteller, *Nat. Rev. Genet.*, 2012, **13**, 679–692.
6 Y. Pan, G. Liu, F. Zhou, B. Su and Y. Li, *Clin. Exp. Med.*, 2018, **18**, 1–14.
7 B. A. Flusberg, D. R. Webster, J. H. Lee, K. J. Travers, E. C. Olivares, T. A. Clark, J. Korlach and S. W. Turner, *Nat. Methods*, 2010, **7**, 461–465.
8 R. Lehmann-Werman, D. Neiman, H. Zemmour, J. Moss, J. Magenheim, A. Vaknin-Dembinsky, S. Rubertsson, B. Nellgrd, K. Blennow and H. Zetterberg, *Proc. Natl. Acad. Sci. U. S. A.*, 2016, **113**, e1826–e1834.
9 M. H. Haque, R. Bhattacharjee, M. N. Islam, V. Gopalan, N. T. Nguyen, A. K. Lam and M. J. A. Shiddiky, *Analyst*, 2017, **142**, 1900–1908.
10 S. Y. Shen, R. Singhania, G. Fehringer, A. Chakravarthy, M. H. A. Roehrl, D. Chadwick, P. C. Zuzarte, A. Borgida, T. T. Wang, T. Li, O. Kis, Z. Zhao, A. Spreafico, T. D. S. Medina, Y. Wang, D. Roulois, I. Ettayebi, Z. Chen, S. Chow, T. Murphy, A. Arruda, G. M. O'Kane, J. Liu,

M. Mansour, J. D. McPherson, C. O'Brien, N. Leighl, P. L. Bedard, N. Fleshner, G. Liu, M. D. Minden, S. Gallinger, A. Goldenberg, T. J. Pugh, M. M. Hoffman, S. V. Bratman, R. J. Hung and D. D. De Carvalho, *Nature*, 2018, **563**, 579–583.

11 Z. Xiong and P. W. Laird, *Nucleic Acids Res.*, 1997, **25**, 2532–2534.

12 Y. Liu, P. Siejka-Zielińska, G. Velikova, Y. Bi and C. X. Song, *Nat. Biotechnol.*, 2019, **37**, 424–429.

13 V. Tryndyak, O. Kovalchuk and I. P. Pogribny, *Anal. Biochem.*, 2006, **356**, 202–207.

14 Z. Dai, T. Cai, W. Zhu, X. Gao and X. Zou, *Chem. Commun.*, 2013, **49**, 1939–1941.

15 O. Taiwo, G. A. Wilson, T. Morris, S. Seisenberger, W. Reik, D. Pearce, S. Beck and L. M. Butcher, *Nat. Protoc.*, 2012, **7**, 617–636.

16 E. J. Wee, T. H. Ngo and M. Trau, *Clin. Epigenet.*, 2015, **7**, 65.

17 A. Jeltsch, J. Broche, C. Lungu and P. Bashtrykov, *J. Mol. Biol.*, 2019, **432**, 1816–1823.

18 C. Grunau, S. J. Clark and A. Rosenthal, *Nucleic Acids Res.*, 2001, **29**, e65.

19 M. Yu, G. C. Hon, K. E. Szulwach, C. X. Song, L. Zhang, A. Kim, X. Li, Q. Dai, Y. Shen, B. Park, J. H. Min, P. Jin, B. Ren and C. He, *Cell*, 2012, **149**, 1368–1380.

20 K. C. Chan, P. Jiang, C. W. Chan, K. Sun, J. Wong, E. P. Hui, S. L. Chan, W. C. Chan, D. S. Hui, S. S. Ng, H. L. Chan, C. S. Wong, B. B. Ma, A. T. Chan, P. B. Lai, H. Sun, R. W. Chiu and Y. M. Lo, *Proc. Natl. Acad. Sci. U. S. A.*, 2013, **110**, 18761–18768.

21 I. Pogribny, P. Yi and S. J. James, *Biochem. Biophys. Res. Commun.*, 1999, **262**, 624–628.

22 C. Gebhard, L. Schwarzfischer, T. H. Pham, R. Andreesen, A. Mackensen and M. Rehli, *Nucleic Acids Res.*, 2006, **34**, e82.

23 K. Inomata, I. Ohki, H. Tochio, K. Fujiwara, H. Hiroaki and M. Shirakawa, *Biochemistry*, 2008, **47**, 3266–3271.

24 M. Frommer, L. E. McDonald, D. S. Millar, C. M. Collis, F. Watt, G. W. Grigg, P. L. Molloy and C. L. Paul, *Proc. Natl. Acad. Sci. U. S. A.*, 1992, **89**, 1827–1831.

25 J. G. Herman, J. R. Graff, S. Myhnen, B. D. Nelkin and S. B. Baylin, *Proc. Natl. Acad. Sci. U. S. A.*, 1996, **93**, 9821–9826.

26 T. R. Church, M. Wandell, C. Lofton-Day, S. J. Mongin, M. Burger, S. R. Payne, E. Castanos-Velez, B. A. Blumenstein, T. Rosch, N. Osborn, D. Snover, R. W. Day, D. F. Ransohoff and I. Presept Clinical Study Steering Committee and T. Study, *Gut*, 2014, **63**, 317–325.

27 T. K. Wojdacz and A. Dobrovic, *Nucleic Acids Res.*, 2007, **35**, e41.

28 J. Antunes, D. S. Silva, K. Balamurugan, G. Duncan, C. S. Alho and B. McCord, *Anal. Biochem.*, 2016, **494**, 40–45.

29 J. Dong, Q. Xu, C. C. Li and C. Y. Zhang, *Chem. Commun.*, 2019, **55**, 2457–2460.

30 H. Zhang, L. Shan, X. Wang, Q. Ma and J. Fang, *Biosens. Bioelectron.*, 2013, **42**, 503–511.

31 W. Zhou, P. W. Laird and H. Shen, *Nucleic Acids Res.*, 2017, **45**, e22.

32 Z. Huang, J. Peng, J. Han, G. Zhang, Y. Huang, M. Duan, D. Liu, Y. Xiong, S. Xia and W. Lai, *Food Chem.*, 2019, **276**, 333–341.

33 H. Kim, D. R. Chung and M. Kang, *Analyst*, 2019, **144**, 2460–2466.

34 X. Liu, C. Zhang, K. Liu, H. Wang, C. Lu, H. Li, K. Hua, J. Zhu, W. Hui, Y. Cui and X. Zhang, *Anal. Chem.*, 2018, **90**, 3430–3436.

35 S. Zhang, Y. Cai, J. Zhang, X. Liu, L. He, L. Cheng, K. Hua, W. Hui, J. Zhu, Y. Wan and Y. Cui, *Nanoscale*, 2020, **12**, 10098–10105.

36 W. Xu, N. Cheng, K. Huang, Y. Lin, C. Wang, Y. Xu, L. Zhu, D. Du and Y. Luo, *Biosens. Bioelectron.*, 2016, **80**, 654–660.

37 G. T. Bommer, I. Gerin, Y. Feng, A. J. Kaczorowski, R. Kuick, R. E. Love, Y. Zhai, T. J. Giordano, Z. S. Qin, B. B. Moore, O. A. MacDougald, K. R. Cho and E. R. Fearon, *Curr. Biol.*, 2007, **17**, 1298–1307.

38 H. Tazawa, N. Tsuchiya, M. Izumiya and H. Nakagama, *Proc. Natl. Acad. Sci. U. S. A.*, 2007, **104**, 15472–15477.

39 D. Lodygin, V. Tarasov, A. Epanchintsev, C. Berking, T. Knyazeva, H. Korner, P. Knyazev, J. Diebold and H. Hermeking, *Cell Cycle*, 2008, **7**, 2591–2600.

40 H. Hermeking, *Cell Death Differ.*, 2010, **17**, 193–199.

41 D. C. Corney, C. I. Hwang, A. Matoso, M. Vogt, A. Flesken-Nikitin, A. K. Godwin, A. A. Kamat, A. K. Sood, L. H. Ellenson, H. Hermeking and A. Y. Nikitin, *Clin. Cancer Res.*, 2010, **16**, 1119–1128.

42 D. Yang, J. Ma, Q. Zhang, N. Li, J. Yang, P. A. Raju, M. Peng, Y. Luo, W. Hui, C. Chen and Y. Cui, *Anal. Chem.*, 2013, **85**, 6688–6695.

43 C. Rohde, Y. Zhang, R. Reinhardt and A. Jeltsch, *BMC Bioinf.*, 2010, **11**, 230.

44 S. Zhang, J. Huang, J. R. Lu, M. Liu and J. S. Zheng, *Curr. Med. Chem.*, 2020, **27**, 6159–6187.

45 M. J. Healey, W. Rowe, S. Siati, M. Sivakumaran and M. Platt, *ACS Sens.*, 2018, **3**, 655–660.

